



## Growth Simulation of Facial/Head Model from Childhood to Adulthood

Alice J. Lin<sup>1</sup>, Shuhua Lai<sup>2</sup> and Fuhua (Frank) Cheng<sup>3</sup>

<sup>1</sup>University of Kentucky, [ajlin0@cs.uky.edu](mailto:ajlin0@cs.uky.edu)

<sup>2</sup>Virginia State University, [slai@vsu.edu](mailto:slai@vsu.edu)

<sup>3</sup>University of Kentucky, [cheng@cs.uky.edu](mailto:cheng@cs.uky.edu)

### ABSTRACT

This paper presents a method to simulate the growth of the facial/head model of a person from childhood to adulthood. The method works by generating continuous data of standard landmarks using auto-regressive moving average based on anthropometry of the head/face. The standard landmarks are assigned to the particular head and face, and vertices of the growing head/facial model are calculated by projecting the vertices to the one dimensional subspace that contains measurements of the landmarks. The vertices of the predicted model are constrained to keep the features of the head/face distinct by grouping vertices into clusters and maintaining each cluster proportionally changing in different age periods. This new technology has applications in security, ID search (for missing children), health care (such as, evaluation of dysmorphic children) and forensic sketch artistry.

**Keywords:** growth, simulation, facial, head, model, childhood, adulthood

**DOI:** 10.3722/cadaps.2010.xxx-yyy

### 1 INTRODUCTION

Due to the growth of the skull, dramatical changes occur in the bony parts of a child face from the neonatal stage to adolescence. Moreover the growth of soft parts changes their thickness and stiffness - a chubby face turns into an elongated and more distinct face during the growth. Additionally, facial features, such as the nose and the eyes, become more prominent and evolve to the main characteristics of a face. All these changes appear slowly and continuously during the growth, this is why it is so difficult to observe and predict the facial changes.

The variability in the shapes of the human head and face is traditionally studied in the field of anthropometry. The literature is rich with insights about the differences in facial proportions among and between various human populations. Extensive statistical data [2] that have been collected over the course of decades are put to use in our methods presented in this paper.

Face Anthropometry is a branch of medical research that deals with measuring and analyzing absolute quantities and proportions of human heads and faces. Traditionally, facial measurements are taken by a medical doctor using an assortment of measuring devices such as rulers, tapes, and goniometers. For precise measurements, a standardized set of landmarks is defined on the head and face. Landmarks are prominent feature points such as the tip of the nose, which can be found by visual examination or palpation. Fig. 1 shows a standard set of landmarks on the face [2]. By redefining the relations between landmarks on the skin according to age-related statistics, facial proportions of a virtual head can be changed, resulting in a plausible model of the same person at a different age. The method of simulating age progression or rejuvenation proposed in this paper supports a multitude of applications: forensic sciences and medicine (clinical diagnostics, operation planning), etc.

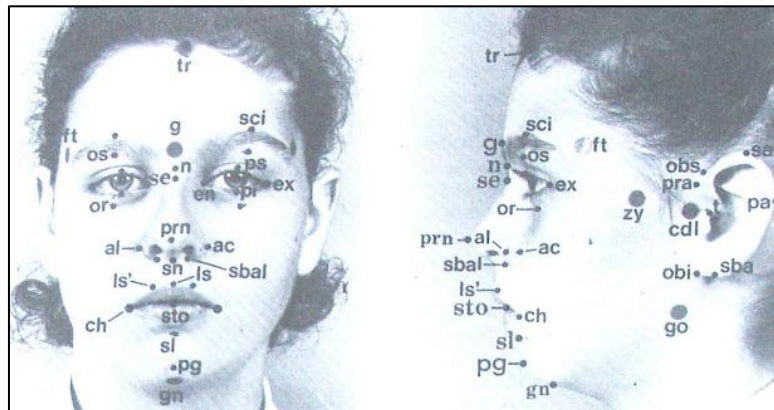


Fig. 1: Landmarks of the head and face in frontal and lateral aspects.

**Clinical diagnostics:** The dimensions of facial structures, their reciprocal spatial positions, and their relative proportions are important components in the clinical analysis and plastic surgery patients. The age progression model allows clinicians to rapidly obtain anthropometric and customized measurements. In the past, doctors used these canons as a reference in the analysis of patients, and approximate conformity with these canons was deemed one of the goals of therapy. The simulating child head and face growth extracts a norm from a population of individuals and can be analyzed for facial features and for evaluation of dysmorphic children. Comparing the standard head and face model with patient data can help to indicate the existence of deformities, possibly leading to discovery of an illness. It is intended to assist in detecting anomalies of the facial growth at early stages of development. Moreover, the autoregressive moving average to predict landmarks makes it possible to describe the individual growth of a head and face continuously, starting from a minimum age of 1 year old to a maximum age of 19 years.

Currently, two-dimensional photographs are most commonly used to facilitate visualization, assessment and treatment of facial abnormalities in craniofacial care but are subject to errors because of perspective, projection, and lack of 3-dimensional information. One can find in the literature a variety of methods to generate 3-dimensional facial images such as laser scans, stereophotogrammetry, infrared imaging and even CT. However each of these methods contains inherent limitations and no system is in common clinical use. There is great interest and demand amongst the craniofacial healthcare community for the use of 3-dimensional models for treatment planning and visualization, and for quantitative assessment of the asymmetry.

**Operation planning:** In the medical field, use of and research on virtual head models concentrates mainly on preoperative planning, for instance, in plastic surgery. If size and shape of a deformity are quantifiable, one can make more exact statements about necessary corrections. The growth-related changes in the head and face help to predict the effect of an operation over several years. For instance, what the long-term effects will be on a rhinoplastic operation can be predicted. For cosmetic surgery - aesthetics and attractiveness of human faces, with the standard head and face model as guide, people

can find generally applicable measurements and proportions for realization of harmonious facial characteristics compatible with sound functionality.

**Forensic application:** A large part of law enforcement work deals with construction, identification, and modification of facial images and models. To this day, this work is largely carried out with the help of skilled artists. When a person, especially a child, went missing, there can be large changes in appearance over time, which may prevent identification due to outdated photographs. Police forces use artificial aging of missing children to increase the chances of finding them after years. To generate age progressed images of children is usually done by a forensic artist based on two-dimensional image processing and infer age-related changes from photographs, relying on anthropometric knowledge and data. The result is an age progressed image to which several haircuts and surrounding conditions can be applied. This kind of processing can also be performed on a 3D model. With the 3D model of the age progressed head and face, we can render arbitrary images of a missing child at any given pose.

The model of age progressing can help in designing health care environments for children. It can assist a designer in determining the scale and placement of features appropriate for different age groups. It also enables the designer to visualize changes in a child, such as aging, and its effect on the usability of devices.

There are many more aspects to growth and aging of heads and faces, such as, changes in skin color, hair growth, wrinkle formation, etc. They will not be covered in the procedure presented here. These parameters can be adjusted manually to accommodate individual and age-related changes.

## 2 RELATED WORK

In contrast to the quantity of medical studies that explain the biological basics of the craniofacial growth in detail, only a few computer aided prediction techniques are available. There are prediction techniques based on the craniofacial development. Nielsen and Andresen [7] presented a mathematical and computational technique for modeling three dimensional growth on human mandibles. The system is based on a data set of computer tomography scans. It diagnoses craniofacial anomaly caused by a genetic defect. The prediction relies on the mandible bone only, no skin surface is estimated. Milner et al. [6] described a method to simulate the aging process of an adolescent skull. To predict an age progressed facial appearance from skull data, the skull model of the current age stage is age progressed first. Afterwards the soft tissue on the skull is simulated with sheet wax, which is applied to the skull. A preliminary CT scan of the head to be studied is essential for the generation of such a synthetic skull.

Kahler et al. [3] presented a construction and deformation method for head models with anatomical structure. The anatomical structure of the face is labeled with a set of anthropometric landmarks. The computation uses only the landmark set, and a warp-technique accomplishes the head deformation. The result is a deformed head, which is fitted to imperfect scan data to simulate head growth from early childhood to adult age. Ramanathan and Chellappa [8] characterized facial growth on two dimensional images by means of growth parameters defined over facial landmarks of individuals under 18 years old. The computational aspects were involved in using face anthropometric data and psychophysical evidences on how humans perceive age progression in faces to develop the proposed craniofacial growth model.

In computer graphics, research on aging in human faces has so far concentrated on the appearance of the skin, neglecting the considerable geometric changes that occur during growth. Lee et al. [5] reconstructed textured low polygon face models from photographs of the members of a family, simulating age changes by blending geometry and textures between young and old family members. Wrinkle patterns are generated semi-automatically by considering muscle fiber orientation and feature points on the face. Tiddeman et al. [11] used wavelet-based methods for prototyping and transforming the facial textures to identify salient features such as age wrinkles in prototype facial images, and apply them to other images to change the apparent age. Suo et al. [9] presented a model for simulating aging process with two dimensional facial images. The model integrates three aspects related to aging changes: global appearance changes in hair style and shape, deformations and aging effects of facial components, and wrinkle appearance at various facial zones.

### 3 OUR APPROACH

To obtain predicted individual head and face models, we use landmarks attached to skin and skull to control the shape of the head and features of the face. Using such anthropometrically meaningful controls enables us to model and create a virtual face that convincingly resembles a real person.

#### 3.1 Generating Landmarks within Age Range

Predicting the future look/shape of a child's face and head is challenging. This is particularly true as the growth of their soft bones changes their head and face structure dramatically. A set of discrete head and face landmarks from one to nineteen years old is provided by Farkas et al. [2]. This is not enough for our work, we need continuous data to construct a standard model of growing children's heads and faces. Each set of landmarks (see Fig. 2) consists of quantitative observations arranged in chronological order. Age is a discrete variable and the chronologically ordered observations might depend on each other. Also, there may be systematic coverage errors in the data time series, in which the errors are often correlated over time. We use autoregressive moving average to predict values of landmark continuously within the age range (see Fig. 3).

$$P_t = \phi_1 P_{t-1} + \phi_2 P_{t-2} + \dots + \phi_p P_{t-p} + e_t - \theta_1 e_{t-1} - \theta_2 e_{t-2} - \dots - \theta_q e_{t-q} \quad (1)$$

The value of the time series,  $P_t$  at time  $t$ , is the sum of the linear regression of its own past and of a moving average, where  $\phi_1, \phi_2, \dots, \phi_p, \theta_1, \theta_2, \dots, \theta_q$  are parameters and  $e_t$  is white noise.  $p$  and  $q$  are degrees of polynomials  $\phi$  and  $\theta$ , respectively.  $\{P_t\}$  denotes the observed time series.  $\{e_t\}$  represents a sequence of identically distributed, zero mean, independent random variables. To estimate the parameters  $\phi$  and  $\theta$ , we begin the recursion at  $t = 2$ . We compute

$$e_t = P_t - \phi_1 P_{t-1} - \phi_2 P_{t-2} - \dots - \phi_p P_{t-p} + \theta_1 e_{t-1} + \theta_2 e_{t-2} + \dots + \theta_q e_{t-q} \quad (2)$$

with start-up values  $e_p = e_{p-1} = \dots = e_{p+1-q} = 0$ . By minimizing the sum of the squares

$SS(\phi_1, \phi_2, \dots, \phi_p, \theta_1, \theta_2, \dots, \theta_q) = \sum_{t=2}^n e_t^2$ , we numerically obtain the least squares estimates of all the parameters  $\phi_1, \phi_2, \dots, \phi_p, \theta_1, \theta_2, \dots, \theta_q$ .

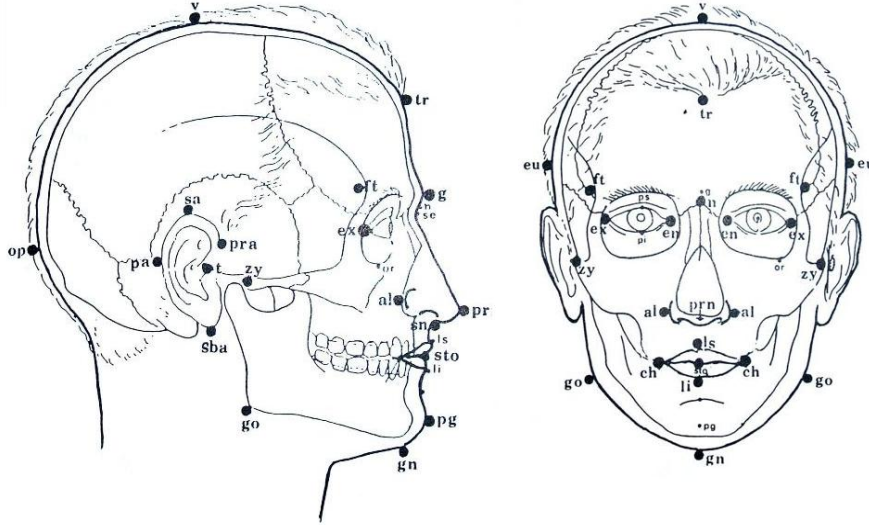


Fig. 2: Landmark set for age-related changes [2].

Fig. 3 is an example of landmarks which represent the mean male craniofacial heights in millimeters from age 1 to 19. The circles are true data. The red line represents predicted height at a given age.

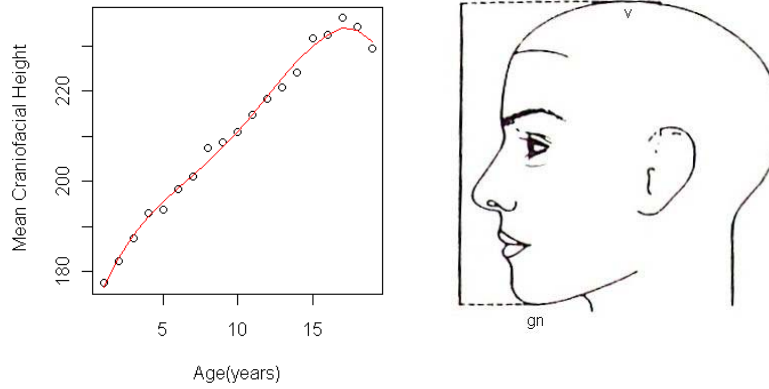


Fig. 3: Mean male craniofacial height (v-gn) from age 1 to 19.

### 3.2 Producing a Particular Child's Landmarks

There are certain noticeable, skeletal and soft tissue age-related shape, size, and configuration changes in individuals. The standard landmarks of a growing child's head and face can predict general ages at which certain changes occur or appear. The particular biological and environmental factors can influence the growth, either delaying or expediting the process. There are also features unique to each individual that can affect the appearance of the growth head and face.

Despite basic anatomical similarities, the small variations in bone structure characterize the individual. To construct a child's head and face model accurately, we assume there is a  $t$  month's 3D child head and face model. We would like to predict the arbitrary  $T$  month's model. For instance, Fig. 4(b) is a mean male width of the head from age 1 to 19. Grey dots are true data [2], and the red curve is a function  $f(x)$  of the landmark (predicted values) for the standard model.  $x$  is time in months.

We have the landmark of a particular child at age  $T$  month:  $m_T = f(t) + \Delta E + D_T$ , that is

$$m_T = f(t) + (f(T) - f(t)) + \frac{m_t - f(t)}{f(t)} * f(T) \quad (3)$$

$m$  is a landmark of a particular child head and face.  $\Delta E$  is the growing effect in standard model for the period from  $t$  to  $T$ .  $D_T$  is the deviation of  $m$  compared with standard model  $f(x)$  at  $T$  months.

### 3.3 Predicting the Vertices of the Model

We assume the whole head is a full space. Each measurement of landmark is a subspace, for example, the measurement of width of the head ( $eu-eu$ ) (see Fig. 4(a), see Fig. 5). The length  $eut$  is half measurement of  $eu-eu$  at time  $t$ . The length  $euT$  is half of length  $eu-eu$  at time  $T$ . The line  $eu-eu$  is a one dimension finite subspace. Each vertex  $v_i$  projects to this space. We have the difference at time  $t$  to  $T$  for  $v_i$  is

$$\vec{\Delta v}_i = \Delta(\vec{v}_i^T - \vec{v}_i^t) = DT - Dt = \left(\frac{euT}{eut} - 1\right)Dt \quad (4)$$

$Dt$  is the distance between the middle of  $eu-eu$  and the point  $v_i$  at time  $t$  projected to  $eu-eu$  subspace (see Fig. 5).  $DT$  is the distance between the middle of  $eu-eu$  and the point  $v_i$  at time  $T$  projected to  $eu-eu$  subspace. We denote the change of  $v_i$  that is subjected to head width  $eu-eu$  as  $\overrightarrow{\Delta v_{eu-eu}}$ . The change of  $v_i$  that is subjected to craniofacial height  $v-gn$  (see Fig. 3) is  $\overrightarrow{\Delta v_{v-gn}}$ . And the changes of  $v_i$  that are affected by head length  $g-op$  (see Fig. 6(a)), nasal tip protrusion  $sn-prn$  (see Fig. 6(b)) and mouth width  $ch-ch$  in Fig. 6(c) are presented as  $\overrightarrow{\Delta v_{g-op}}$ ,  $\overrightarrow{\Delta v_{sn-prn}}$  and  $\overrightarrow{\Delta v_{ch-ch}}$  respectively. The difference of a vertex from time  $t$  to  $T$  is the sum of differences of this vertex projected to all subspaces. The  $i^{th}$  vertex at time  $T$  is:

$$\overrightarrow{v_{i,T}} = \overrightarrow{v_{i,t}} + \overrightarrow{\Delta v_{i,eu-eu}} + \overrightarrow{\Delta v_{i,v-gn}} + \overrightarrow{\Delta v_{i,g-op}} + \overrightarrow{\Delta v_{i,sn-prn}} + \overrightarrow{\Delta v_{i,ch-ch}} + \dots \quad (5)$$

If the vertex projection falls outside of the subspace, it is considered that the landmark has no effect on the vertex.

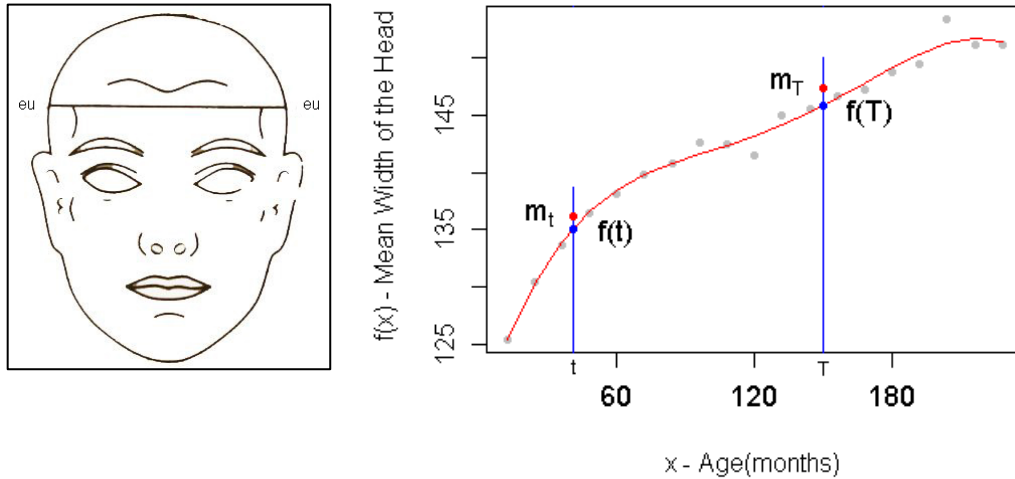


Fig. 4: (a) Width of the head ( $eu-eu$ ), (b) Mean width of the head from age 1 to 19.

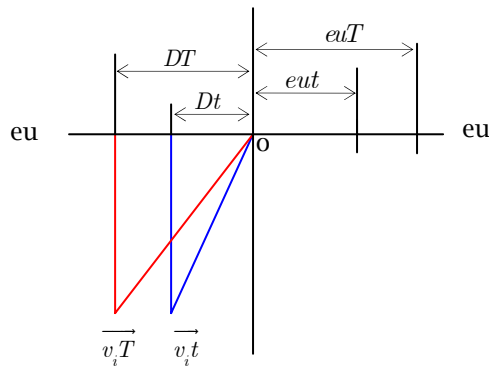


Fig. 5: A vertex project to subspace  $eu-eu$  at time  $t$  and  $T$ .

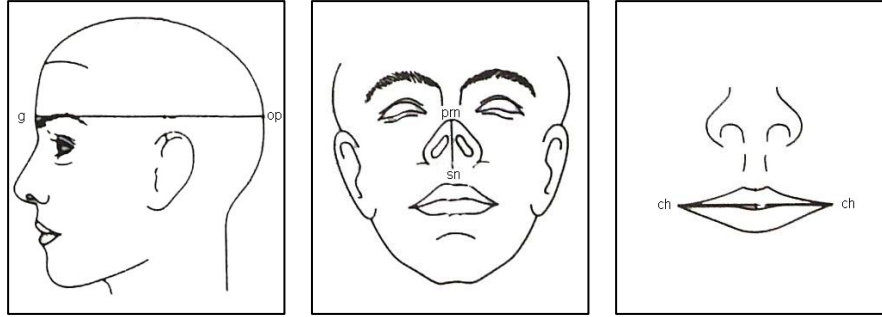


Fig. 6: (a) Length of the head ( $g-op$ ), (b) Nasal tip protrusion ( $sn-prn$ ), (c) Width of the mouth ( $ch-ch$ ).

### 3.4 Constraining the Predicted Vertices

Every child's face is unique. To keep the child facial features distinct, we group the vertices into clusters, and maintain a proportional change of each cluster in different age periods.

First we classify the vertices of the model as the tree based on univariate splits of predictor variables. The resulting splits yield the same predicted classes for the vertices. The V-fold cross-validation [1] is chosen to optimize the tree size (clusters in the data). Once we have determined the initial number of clusters, iterative relocation is used to improve the clustering and attempt to find the best number of clusters, which are represented by their centroids [10]. The process iterates until the criterion function converges. Typically, the square-error criterion is used. This criterion tries to make the resulting  $K$  clusters as compact and as separate as possible. We calculate the error at each data point (i.e. its Euclidean distance to the closest centroid) and then compute the total

sum of the squared errors. 
$$SSE = \sum_{i=1}^K \sum_{v \in C_i} dist(c_i, v)^2$$
 Where  $v$  is a vertex;  $C_i$  is the  $i^{th}$  cluster;  $c_i$  is the

centroid of cluster  $C_i$ ;  $K$  is the number of clusters;  $dist$  is the standard Euclidean distance between two vertices. The best centroid for minimizing the SSE of a cluster is the mean of the points in the cluster. The centroid of the  $i^{th}$  cluster is  $c_i = \frac{1}{m_i} \sum_{v \in C_i} v$ ,  $m_i$  is the number of vertices in the  $i^{th}$  cluster.

Fig. 7(a) is an example of colored clusters of head and face. The vertices in different color belong to different clusters. The vertices in the orange cluster in Fig. 7 (b) will be constrained in the positions which make the cluster proportionally change during nose growth.

Fig. 8 is an example of a Caucasian boy in different ages. Craniofacial norms for Caucasian child [2] were referenced. Fig. 9 is an example of an African-American boy and Fig. 10 is an Asian (Chinese) boy. Craniofacial norms for African-American child [4] and for Chinese child [2] are referenced respectively.

## 4 DISCUSSION AND CONCLUSION

A new approach to simulate the growth of a child's head and face is presented. Landmark-based anthropometric measurement data are used to control growth. Feature based clustering of vertices and proportional change within each cluster ensure feature preserved growth of the predicted model from infancy to adulthood. The anthropometric measurement plays a cornerstone role for simulating the growth of the facial/head model. The development of the human physical body has been changed from time to time. It is important to gather and analyze recent anthropometric data of diverse human populations. The predicted model will be more accurate if the anthropometric data is in the same era. We hope in the future the new anthropometric data will appear, and that will make our proposed method more promising. Most studies only consider ages up to maturity at age 18. At this point, head

growth is considered to be settled. It may change in post-adolescent years and the head and facial dimensions may increase continuously throughout the life span. We will extend our method to adult aging and we expect to see more applications of our method to other field.

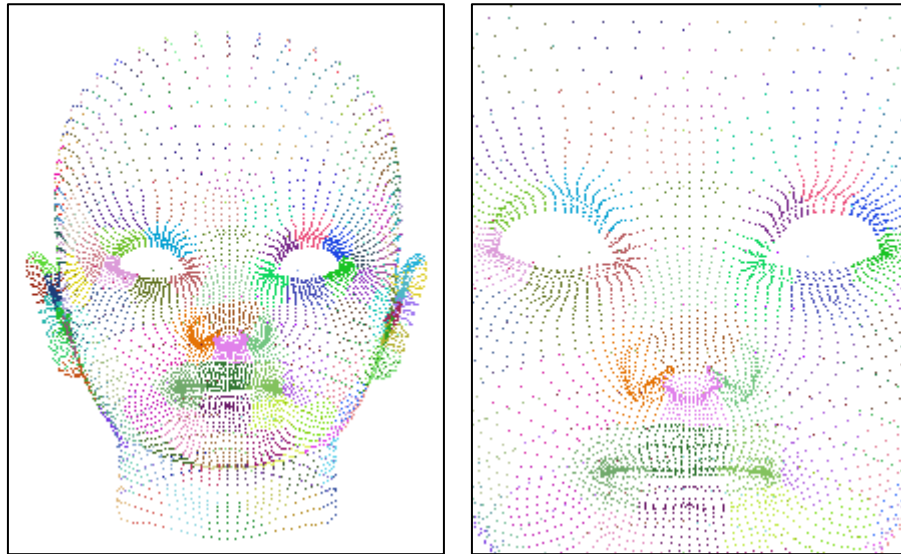


Fig. 7: Colored clusters of head and face.

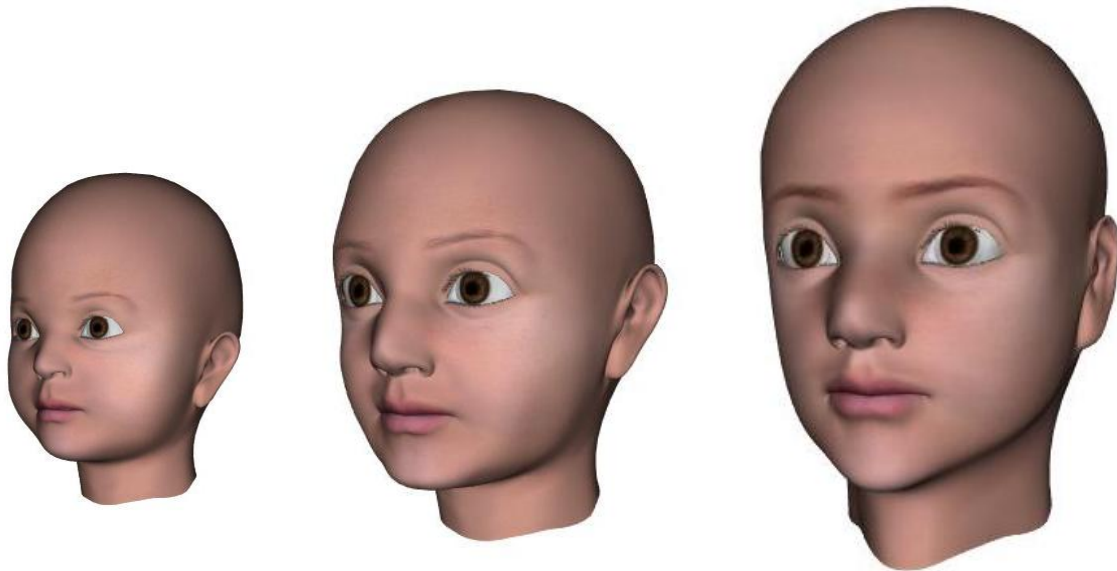


Fig. 8: A Caucasian boy at different ages.

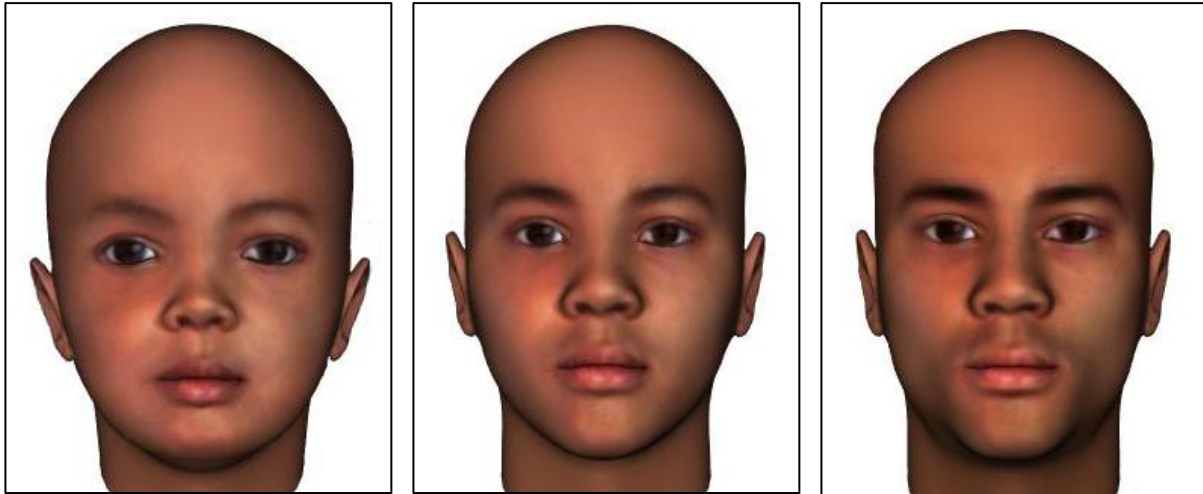


Fig. 9: An African-American boy at different ages.

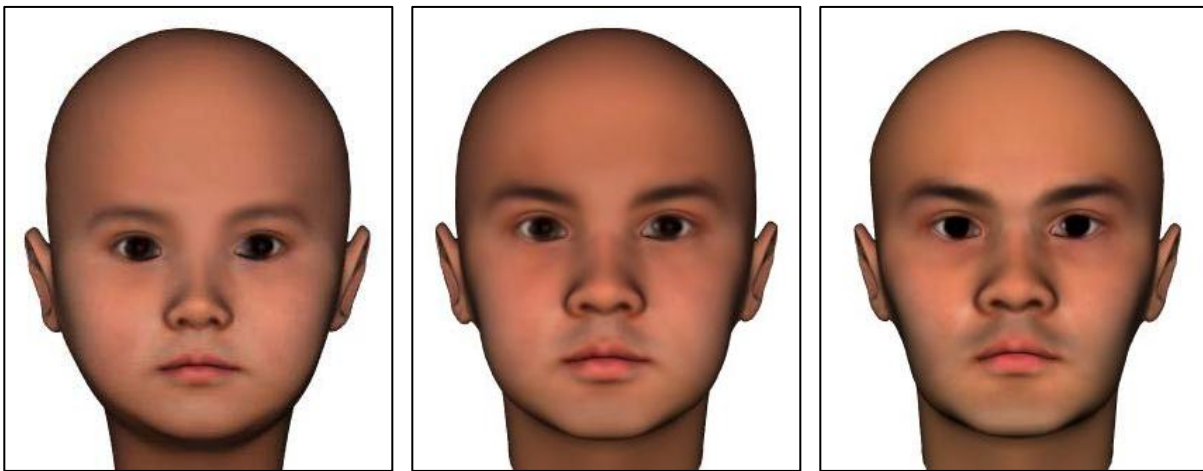


Fig. 10: An Asian (Chinese) boy at different ages.

#### REFERENCES

- [1] Burman, P.: A comparative study of ordinary cross-validation, v-fold cross-validation and the repeated learning-testing methods, *Biometrika*, 76(3), 1989, 503-514.
- [2] Farkas, L. G.: *Anthropometry of the head and face*, Raven Press, New York, NY, 1994, 2nd ed.
- [3] Kahler, K.; Haber, J.; Yamauchi, H.; Seidel, H.: *Head Shop: Generating Animated Head Models with Anatomical Structure*, ACM Siggraph Symposium on Computer Animation, 2002, 55-64.
- [4] Krogman, W. M.: Growth of head, face, trunk, and limbs in Philadelphia white and negro children of elementary and high school age, *Monographs of the Society for Research in Child Development*, 35(3), 1970, 48-80.
- [5] Lee, W.-S.; Wu, Y.; Magnenat-T., N.: Cloning and Aging in a VR Family, *IEEE Virtual Reality Conference*, 1999, 61-68.

- [6] Milner, C. S.; Neave, R. A.; Wilkinson, C. M.: Predicting growth in the aging craniofacial skeleton, <http://www.fbi.gov/hq/lab/fsc/backissu/july2001/milner.htm>.
- [7] Nielsen, M.; Andresen, P. R.: Feature displacement interpolation, *International Conference on Image Processing*, 3, 1998, 208-212.
- [8] Ramanathan, N.; Chellappa, R.: Modeling Age Progression in Young Faces, *Proceedings of Conference on Computer Vision and Pattern Recognition*, 1, 2006, 387-394.
- [9] Suo, J.; Min, F.; Zhu, S.; Shan, S.; Chen, X.: A Multi-Resolution Dynamic Model for Face Aging Simulation, *Conference Computer Vision and Pattern Recognition*, 17(22), 2007, 1-8.
- [10] Tan, P.-N.; Steinbach, M.; Kumar, V.: *Introduction to Data Mining*, Addison Wesley, 2006.
- [11] Tiddeman, B.; Burt, M.; Perrett, D.: Prototyping and Transforming Facial Textures for Perception Research, *IEEE Computer Graphics and Applications*, 21(5), 2001, 42-50.